

Functional characterization of *C. elegans* Y-box-binding proteins reveals tissue-specific functions and a critical role in the formation of polysomes

Andreas Arnold^{1,2}, Md Masuder Rahman³, Man Chun Lee³, Sandra Muehlhaeuser¹, Iskra Katic¹, Dimos Gaidatzis^{1,5}, Daniel Hess¹, Claudia Scheckel^{1,2}, Jane E. Wright¹, Attila Stetak⁴, Peter R. Boag³ and Rafal Ciosk^{1,*}

¹Friedrich Miescher Institute for Biomedical Research, Basel 4058, Switzerland, ²University of Basel, Petersplatz 1, CH-4003 Basel, Switzerland, ³Department of Biochemistry and Molecular Biology, Monash University, Victoria 3800, Australia, ⁴Department of Neuroscience, Biozentrum/Pharmazentrum, Basel 4046, Switzerland and ⁵Swiss Institute of Bioinformatics, CH-4058 Basel, Switzerland

Received July 03, 2014; Revised October 02, 2014; Accepted October 17, 2014

ABSTRACT

The cold shock domain is one of the most highly conserved motifs between bacteria and higher eukaryotes. Y-box-binding proteins represent a subfamily of cold shock domain proteins with pleiotropic functions, ranging from transcription in the nucleus to translation in the cytoplasm. These proteins have been investigated in all major model organisms except *Caenorhabditis elegans*. In this study, we set out to fill this gap and present a functional characterization of CEYs, the *C. elegans* Y-box-binding proteins. We find that, similar to other organisms, CEYs are essential for proper gametogenesis. However, we also report a novel function of these proteins in the formation of large polysomes in the soma. In the absence of the somatic CEYs, polysomes are dramatically reduced with a simultaneous increase in monosomes and disomes, which, unexpectedly, has no obvious impact on animal biology. Because transcripts that are enriched in polysomes in wild-type animals tend to be less abundant in the absence of CEYs, our findings suggest that large polysomes might depend on transcript stabilization mediated by CEY proteins.

INTRODUCTION

The cold shock domain (CSD) is one of the most ancient and highly conserved protein domains known, sharing more than 40% identity and 60% similarity between bacteria and vertebrates (1). This nucleic acid binding motif enables the proteins to bind to both ssRNA and/or ss-

DNA (2). A small subgroup of the CSD protein superfamily includes the so-called Y-box-binding proteins (YBPs). Apart from the CSD, YBPs can contain additional motifs, such as basic/aromatic or glycine-rich stretches in vertebrate and plant proteins, respectively, and RG/RGG repeats in a range of invertebrate proteins (1,3). Even though YBPs act predominantly as nucleic acid binding proteins, they can also directly interact with other proteins, as has been shown for human YB-1 (4). These interactions usually depend on motifs located outside the CSD. YB-1, for example, binds to actin filaments via its alanine- and proline-rich N-terminal domain (5).

Previous work from many laboratories revealed that YBPs function in different cellular processes, best represented by the intensively studied human YB-1 (reviewed in (4)). In the nucleus, for instance, this protein is involved in transcription, DNA repair and pre-mRNA splicing, while in the cytoplasm it has an important role in mRNA regulation, which includes both mRNA stability and translation repression or activation. Another family member, FRGY-2, is expressed specifically in *Xenopus* oocytes. Its main function is to package newly synthesized maternal messages and keep them stable and translationally inactive until needed (6–8). Further examples of YBPs with important functions in the germline are MSY-2, which is important for the stability of many maternally provided mRNAs in mice (9,10), Yps, which plays a role in correct localization and expression of maternal oskar mRNA in *Drosophila* (11), and Ybx1, which regulates maternal sqt1 mRNA translation and thereby ensures correct development of the zebra fish embryo (12). Due to their ability to bind and package mRNA, YBPs have also been referred to as ‘RNA histones’ (1). Just like YBPs, the so-called

*To whom correspondence should be addressed. Tel: +41 61 697 5203; Fax: +41 61 697 3976; Email: rafal.ciosk@fmi.ch

DEAD-box helicases appear to be common constituents of mRNA/protein granules (RNPs) and it has been suggested that these enzymes help to establish and stabilize the interaction of YBPs with ssRNA (13). A previous study identified *Caenorhabditis elegans* YBPs (CEYs) as interaction partners of the DEAD-box helicase CGH-1 (14), which is essential for correct oogenesis (15). The abnormal oocytes that form in the *ceh-1* mutant appear in part to be a result of the formation of large aberrant RNP granules (16–18), which have been proposed to represent solid aggregates of abnormal RNPs (19).

Here, we present a comprehensive characterization of CEYs that expands our understanding of the function of these proteins in animal biology. We show that CEYs are essential for the production of viable progeny and have a conserved role in the formation of maternal mRNPs. Additionally, we present an unexpected function of these proteins in the soma. We find that, in the absence of CEYs, there is a spectacular loss of large polysomes with the concomitant increase of mono- and disomes, suggesting that CEYs are essential for the proper accumulation of multiple ribosomes on mRNAs. Surprisingly, however, this loss of large polysomes appears to have little consequences for animal development and homeostasis. The potential roles of CEYs in polysome biogenesis and in animal biology are discussed.

MATERIALS AND METHODS

Culturing animals

Animals were usually grown on 3.5–15 cm NG 2% plates seeded with OP50 bacteria. For large-scale experiments, animals were grown on 15 cm peptone-rich plates seeded with OP50 bacteria. Gravid adults were then bleached and allowed to hatch on empty plates o/n. The next morning, synchronized L1s were counted and a defined number of larvae were transferred to seeded plates. Animals were then grown to young adulthood and harvested in liquid N₂. The two temperature-sensitive strains, *glp-1(e2144)* and *glp-4(bn2)*, were maintained and grown to large numbers at 15°C, before bleaching gravid adults and then shifting staged L1s to 25°C.

Strains

cey-1(ok1805), *cey-2(ok902)*, *cey-4(ok858)*, *glp-1(e2144)*, *glp-4(bn2)*, *efk-1(ok3609)*, *ced-9(n1950)* and *ced-1(e1735)* mutants were obtained from CGC. The *cey-3(tm2839)* mutant was provided by the Mitani Lab through the National Bio-Resource Project of the MEXT, Japan. All strains were outcrossed at least 4× before use. The AIR-2-GFP transgenic line was provided by the Colaiácovo Lab (20). Transcription activator like effector nucleases (TALENs) (21,22) were used to delete *cey-3* in the *cey-2* mutant background to obtain the *cey-2,-3* double mutant. A common cross of the two single mutants was not attempted due to very close proximity of the two genes (<0.1 cM). We obtained an 8-bp deletion in the first exon, which created a premature stop codon soon after, making this *cey-3(rrr11)* mutant a functional null (confirmed by sterile phenotype of the *cey-1,-2,-3,-4* mutant).

Despite a 539-bp deletion, the *cey-1(ok1805)* mutant still gave rise to a severely truncated version of CEY-1. This protein contained the first part of the cold shock domain with both RNA-binding motifs (RNP1 and RNP2) (2,23). Due to unpredictable effects of such a protein, we used the Cas9/CRISPR system to obtain a functional null mutant (24). We obtained a 5-bp deletion in the second exon that generated a premature stop codon soon after. The aberrant transcript was recognized and degraded by the NMD pathway (confirmed by semi-quantitative PCR).

Transgenic lines

Multisite Gateway (Life Technologies) was used to clone almost all transgenes. Only CEY-3-GFP was obtained from the TransgeneOme project (25). For the expression of FLAG-tagged CEY-4, the ubiquitous *dpy-30* promoter had to be used instead of the endogenous *cey-4* promoter (also ubiquitous) due to technical problems during cloning. An operon system (26) was used to monitor expression of FLAG-tagged transgenes. Supplementary Table S1 shows a list of transgenes generated for this study. Except for CEY-3-GFP, which was obtained by bombardment, all transgenic lines were obtained using MosSCI (27). Each line was outcrossed at least 2× before use.

RNAi

Young adult hermaphrodites were injected with *cey-2,-3* dsRNA (500 ng/μl each). Injected animals were allowed to lay eggs for 10–12 h, before being transferred to new plates and grown at 25°C. *ceh-1* RNAi was performed by feeding (28).

Counting progeny numbers

For each strain, 10 L1s were picked to individual plates and grown to adulthood at the corresponding temperature (20°C, 25°C or 26°C). Adults were picked every 24 h to new plates (two to three times). This allowed for a more accurate counting of the progeny number.

Microscopy

Images were captured with a Zeiss AxioImager Z1 microscope, equipped with an AxioCam MRm REV2 CCD camera. All images were acquired in the linear mode of the Axiovision software (Zeiss) and processed using Image J and Adobe Photoshop CS4 in an identical manner.

Live imaging

Animals were transferred into a drop of 0.04 M levamisol on an agarose pad, covered with a cover slip and immediately imaged.

Cell death assays

To measure germ cell death, animals were incubated for 3–4 h on NGM plates containing acridine orange (AO) (500 μl of 100 mM AO/plate) and viewed by fluorescent microscopy (14). Cell corpses were counted visually using DIC optics.

Immunostaining

Immunostaining was performed as previously described (15). The following primary antibodies were used: α -CEY-4 (Supplementary Figure S1), α -GLD-1 (29), α -CGH-1 (14), α -CAR-1 (14), α -pH3 (phospho-histone H3) (Upstate Biologicals) and α -activated MAPK-YT (Sigma). DNA was visualized using 4',6-Diamidino-2-phenylindole (DAPI).

RNA extraction

One milliliter of Trizol (Life Technologies) was added to each frozen *C. elegans* pellet (50–200 μ l) and then ground using a mortar and pestle in the presence of liquid N₂. Extracts were centrifuged at 4°C for 10 min at 12 000 \times g to get rid of remaining debris. Supernatants were transferred to new microcentrifuge tubes and 200 μ l of chloroform were added, vortexed for 0.5 min and then centrifuged at 4°C for 15 min at 12 000 \times g. The aqueous phase was transferred to a new microcentrifuge tube and 500 μ l of isopropanol were added, mixed well and incubated at RT for 15 min. The samples were then centrifuged at 4°C for 10 min at 12 000 \times g. Subsequently, the RNA pellet was washed once with 75% ethanol, before being air dried and resuspended in nuclease-free water (Ambion). To obtain germline-specific RNA, gonads were manually dissected and RNA was purified using the Arcturus PicoPure RNA Isolation Kit (Life Technologies).

DNA and rRNA removal

DNase treatment was performed with RNeasy Mini columns (Qiagen) using the corresponding RNase-free DNase set (Qiagen). The RNA cleanup protocol was followed. Removal of rRNA was performed using the RiboZero™ Magnetic Gold Kit (Human/Mouse/Rat, Epicentre). For qRT-PCR, RNA samples were only DNase treated. For total RNA sequencing, RNA samples were DNase treated and rRNA was removed. rRNA removal was checked on the Agilent Bioanalyzer using the Pico RNA chip.

qRT-PCR

Reverse transcription reactions were performed using the ImProm-II Reverse Transcription System (Promega) using random primers (Promega). For subsequent qRT-PCR reactions, one primer in each pair overlapped an exon-exon junction to avoid amplification from non-mRNA molecules.

Polysome profiling

Polysome profiling and RNA extraction from sucrose fractions was performed as previously described (30). A 15% (w/v) to 60% (w/v) sucrose gradient was used for polysome profiles shown (each profile was obtained at least twice). For ribosome profiling, a 5% (w/v) to 45% (w/v) sucrose gradient was used.

Ribosome profiling

Nematode lysates were prepared as described for polysome profiling (30), however, without adding RNase inhibitor to the lysis buffer. RNase I (200 U/110 OD, Ambion) was added and the mixture was incubated at 23°C for 1 h. The remaining extract was used for total RNA extraction for subsequent total RNA sequencing. After digestion, the lysate was immediately loaded on the gradient and centrifuged. Samples were then fractionated into 24 collection tubes instead of the usual 12. This allowed cleaner isolation of monosomes. Ribosome-protected fragments (RPFs) were then isolated as described above for total RNA extraction. RNA was loaded on a Novex 15% TBE-Urea gel (Life Technologies) and a piece between 27 and 31 nt (oligos from Genscript) was excised from the gel and the RNA was eluted from the gel piece o/n at RT. The library was then prepared using the TruSeq Small RNA kit (Illumina), whereby the RNA was precipitated for at least 4 h in between each of the following steps. RNA was first dephosphorylated using T4 PNK (NEB), followed by 3' adapter ligation (T4 RNA ligase 2 truncated, NEB). The 5' end was then re-phosphorylated using T4 PNK (NEB) supplied with ATP, followed by 5' adapter ligation, cDNA synthesis and PCR. The PCR product was then loaded on a Novex 6% TBE-Urea gel (Life Technologies) and the band around 150 bp (5' adapter + 30 nt RPF + 3' adapter) was excised from the gel. The DNA was then eluted from the gel piece and sent for sequencing.

RNA sequencing and data analysis

For total RNA sequencing, the samples were prepared using the ScriptSeq™ v2 RNA-Seq Library Preparation Kit (Epicentre) and then sequenced. Both the total RNA sequencing data and the ribosome profiling data were analyzed as previously described (31).

Microarray and data analysis

Sample preparation, microarray and subsequent data analysis were performed in the *glp-4(bn2)* mutant as previously described for wild-type (29).

Western blot analysis and antibodies used

Depending on the pellet size, 300–600 μ l extraction buffer (50 mM HEPES, 100 mM KOAc, 5 mM MgAc, 0.1% Triton X-100, 10% Glycerol (w/v), 20 mM β -glycerophosphate) were added to the pellet. Protein extracts were then prepared as for RNA extraction by grinding with a mortar and pestle in the presence of liquid N₂. Animal debris were removed by a 20-min spin at 20 000 \times g. Protein concentrations were measured using the Bradford assay (Biorad). The required amounts of 4 \times LDS sample buffer (Life Technologies) and 10 \times sample reducing agent (Life Technologies) were added to the samples, followed by 10 min of heating at 70°C. The samples were then loaded on a gel (NuPAGE Novex 4–12% Bis-Tris Protein Gels, 1.0 mm, 10 well or 17 well) and ran for 55 min at 200 V. Proteins were transferred to the membrane using the Trans-Blot® Turbo™ system (Biorad). Membranes were then washed 2 \times 10 min in

ddH₂O, Ponceau stained for 5–10 min and cut if necessary. After washing for 2 × 5 min with PBS-T (Tween 1:1000), membranes were blocked with 4% milk (in PBS-T) for 1 h. The primary antibody was then added. The primary α-PAB-1 (29), α-CEY-4 (Supplementary Figure S1), α-RME-2 (32), α-ACT-1 (MAB1501, Millipore), α-EEF-2 (Cell Signaling Technology) and α-EEF-2-P (Cell Signaling Technology) antibodies were incubated o/n at 4°C. The next day, membranes were washed 3 × 5 min in 4% milk (in PBS-T) before the secondary (HRP-coupled) antibody was applied (GE Healthcare) for 1 h at RT. The membranes were then washed 3 × 5 min in PBS-T and then developed using Pierce ECL Western Blotting Substrate (Thermo Scientific). For FLAG detection, we used the primary monoclonal ANTI-FLAG[®] M2-Peroxidase (HRP) antibody (Sigma). This antibody is coupled to HRP. After 2 h of incubation at RT, the membrane was washed 3 × 5 min in PBS-T and then developed using Pierce ECL Western Blotting Substrate (Thermo Scientific).

Protein extraction from sucrose fractions

One hundred and fifty microliters from each sucrose fraction were transferred to a new 1.5 ml microcentrifuge tube and filled up with washing buffer (20 mM Tris-HCl pH 7.9, 140 mM KCl, 5 mM MgCl₂) to 500 μl. The entire volume was then loaded onto an Amicon Ultra-0.5 Centrifugal Filter Unit (Millipore) and centrifuged at 4°C for 30 min at 14 000 × g. A 7 μl 4× LDS sample buffer (Life Technologies) and 3 μl 10× sample reducing agent (Life Technologies) were added to each sample (17 μl), which was then heated at 70°C for 10 min. Subsequently, 14 μl were loaded on the gel.

Surface sensing of translation (SUnSET)

L1s were hatched in M9 o/n at 150 rpm. Per sample, 12 000 L1s were grown to young adulthood on NG 2% plates seeded with OP50 bacteria. Animals were washed off the NG 2% plates and washed twice in S-basal (33). Four milliliters of S-medium (33) were added to the animals and transferred to a 50 ml Erlenmeyer. An o/n culture of OP50 bacteria was 10× concentrated and the pellet was resuspended in S-medium. Seven hundred and fifty microliters of bacteria solution were added to the Erlenmeyer. Finally, 250 μl of puromycin stock solution (10 mg/ml) were added, resulting in a final volume of 5 ml and a final puromycin concentration of 0.5 mg/ml. Animals were grown in the presence of puromycin for 4 h at 200 rpm and then harvested. Four hours allowed detection of a puromycin signal by western blot analysis, without having an obvious effect on general translation (no abnormalities observed on polysome profiles, data not shown). Fifty micrograms of total protein were loaded per well for western blot analysis. This allowed for a good signal at a reasonable exposure time of 5–10 min. The monoclonal α-puromycin antibody (Millipore, (34)) was used at a dilution of 1:5000 in 4% milk (in PBS-T). For GFP detection, we used monoclonal GFP antibodies (Roche). GFP (GFP-RPS-1) was used as a spike and served as an external loading control.

³⁵S-methionine incorporation assay

The assay was performed as previously described (35).

CEY-1 and CEY-4 immunoprecipitation and mass spectrometry (MS) analysis

CEY-1 and CEY-4-associated proteins were identified by anti-FLAG IPs, using FLAG-coupled Dynabeads (Life Technologies). The FLAG IPs were performed on FLAG-CEY-1 and FLAG-CEY-4 transgenic lines, and wild-type. An on-bead RNase digestion was performed with 0.1 mg/ml RNase A (Sigma) for 2 h at 4°C. After washing, samples were eluted using FLAG peptides (Sigma). Samples were TCA precipitated and submitted for MS. The protein pellets were dissolved in 0.5 M Tris pH 8.6, 6 M guanidinium hydrochloride, reduced with 16 mM TCEP for 30 min and alkylated in 35 mM iodoacetamide for 30 min in the dark. The proteins were digested with 0.2 μg Lys-C (Wako chemicals, Osaka, Japan) for 6 h after 3× dilution in 50 mM Tris 5mM CaCl₂ (pH 7.4), followed by 0.2 μg trypsin after an additional 2× dilution, overnight. The peptides were analysed by capillary liquid chromatography tandem MS with an EASY-nLC 1000 using the two-column setup (Thermo Scientific). The peptides were loaded in buffer A onto a peptide trap (Acclaim PepMap 100, 75 μm × 3 cm, C18, 3 μm, 100 Å) at a constant pressure of 500 bar. Then they were separated, at a flow rate of 200 nl/min with a gradient of 2–44% buffer B in buffer A in 67 min (buffer A: 0.1% formic acid in water, buffer B: 0.1% formic acid in acetonitrile) using a 75 μm × 25 cm Reprosil-PUR C18, 3 μm, 100 Å PicoFrit column mounted on a DPV ion source (New Objective). The data were acquired on an Orbitrap Velos (Thermo Scientific) using 60 000 resolution for the peptide measurements in the Orbitrap and a top 20 method with CID fragmentation and fragment measurement in the LTQ, according to the recommendation of the manufacturer. Mascot (Matrix Science, London, UK) searching UniProt database version 2012.09 was used to identify the peptides. The enzyme specificity was set to trypsin allowing for up to three incomplete cleavage sites. Carbamidomethylation of cysteine (+57.0245) was set as a fixed modification, oxidation of methionine (+15.9949 Da), acetylation of protein N-termini (+42.0106 Da), dimethylation of Arginine (+28.0312 Da) and phosphorylation of Serine and Threonine (+79.9663) were set as variable modifications. Parent ion mass tolerance was set to 5 ppm and fragment ion mass tolerance to 0.6 Da. The results were validated with the program Scaffold Version 4.0 (Proteome Software, Portland, USA). Peptide identifications were accepted if they could be established at greater than 50% probability as specified by the Peptide Prophet algorithm (36). Protein identifications were accepted if they could be established at greater than 95% probability and contained at least two identified peptides. Protein probabilities were assigned by the Protein Prophet algorithm (37). Post-translational modification sites were further evaluated with the software ScaffoldPTM 2.1.2.1 (Proteome Software) and validated manually. Relative quantification of the proteins was done with the program ProgenesisLC (Nonlinear Dynamics).

Phylogenetic tree

Protein sequences (fasta files) were obtained from www.uniprot.org. Sequence alignment and phylogenetic tree were constructed using Clustal Omega (<http://www.ebi.ac.uk/Tools/msa/clustalo/>). Njplot (<http://pbil.univ-lyon1.fr/software/njplot.html>) was used to modify the phylogenetic tree.

Chemotaxis

Chemotaxis was tested toward different volatile chemo-attractants as described (38). Briefly, animals were given a choice between a spot of 0.1% (vol/vol) attractant in ethanol with 20 mM sodium-azide and a counter spot with ethanol and sodium-azide. After 1 h, the animals were counted and a chemotaxis index was calculated as described (38). Fifty to two hundred synchronized young adults were used per plate and each experiment was done in triplicates and repeated three times.

Olfactory conditioning and memory

Olfactory conditioning and memory was assessed as described previously (39). Starvation conditioning was performed using young adult animals on conditioning plates without food in the presence of 2 μ l undiluted diacetyl spotted on the lid and trained for 1 h on 10 cm CTX plates (5 mM $\text{KH}_2\text{PO}_4/\text{K}_2\text{HPO}_4$ pH = 6.0, 1 mM CaCl_2 , 1 mM MgSO_4 , 2% agar). Naive and conditioned animals were given a choice between a spot of 0.1% (vol/vol) DA in ethanol with 20 mM sodium-azide and a counter spot with ethanol and sodium-azide for 1 h, and chemotaxis index was calculated as described (38). Memory was assessed as described (40) where diacetyl conditioned animals were tested for their preference toward the attractant following a 60-min resting period in absence of food and odorant.

RESULTS

CEYs are ubiquitous cytoplasmic proteins

The *C. elegans* genome encodes five CSD-containing proteins, which include the well-studied developmental regulator LIN-28 (41,42) and four previously uncharacterized proteins, CEY-1-4, which are the focus of this study. CEYs are relatively small proteins, ranging from around 200 amino acids (CEY-1) to almost 300 amino acids (CEY-4). CEY-2 and CEY-3 are around 270 amino acids in length and are 70% identical. As their expression patterns also overlap (see below), CEY-2 and CEY-3 very likely have redundant functions. The CSD represents one of the most highly conserved protein domains (1). However, outside the CSD, CEYs share only limited similarity with YBPs from other species (Figure 1A). In addition to the CSD, CEY-1 and CEY-4 contain RG/RGG repeats (Figure 1B), which is reminiscent of such repeats in other invertebrate YBPs (43–45).

To find out where the different *cey* genes are expressed, we generated GFP reporters. The results revealed that *cey-1* and *cey-4* were present in both the soma and the germline, whereas *cey-2* and *cey-3* were only expressed in the germline

(Figure 1C and D). This was confirmed by qRT-PCR performed on RNA isolated from either wild-type animals or temperature-sensitive *glp-4(bn2)* mutants, which, when grown at 25°C, have no germline (Supplementary Figure S2A). In addition, the reporters revealed that *cey-2* and *cey-3* were lowly expressed in the distal most part of the gonad that contains self-renewing undifferentiated germ cells, but became strongly expressed upon the entry of germ cells into meiosis (Figure 1C and D). Furthermore, we observed the disappearance of GFP-tagged versions of CEY-2 and CEY-3 during the oocyte-to-embryo transition, such that these proteins were no longer detected in early embryos (Figure 1E).

YBPs in other organisms have been implicated in gene regulation at both transcriptional and post-transcriptional levels. Accordingly, they are present in both the cytoplasm and the nucleus, best illustrated by the human YB-1 (4). In contrast, immunostaining and GFP localization experiments showed that CEY proteins were only present in the cytoplasm in both soma and germline (Figure 1E and Supplementary Figure S2B). Knockdown of *xpo-1*, the homolog of yeast, vertebrate and *Drosophila* CRM1/exportin-1, which represents the major receptor for the export of proteins out of the nucleus (46), did not cause an accumulation of CEY-1 or CEY-2 in the nucleus (data not shown). This supports a predominantly cytoplasmic localization for CEYs, allowing the analysis of post-transcriptional roles of these proteins independently from potential functions in the nucleus, for example, in transcription or mRNA splicing.

Both CEY-1 and CEY-4 contain RG/RGG repeats. The arginine residues can serve as targets for protein arginine methyl transferases (PRMTs), which can either mono- or di-methylate arginines and thereby alter protein function (47). Our MS data (data not shown) suggested that some of the RG/RGG repeats were indeed methylated and western blotting experiments confirmed this, showing that both CEY-1 and CEY-4 were asymmetrically dimethylated (ADMA) (Supplementary Figure S2C and D). The RG/RGG methylation was recently shown to depend on PRMT-1 in *C. elegans* (48). Consistently, we found that CEY-4 no longer carried the ADMA mark in the *prmt-1(ok2710)* mutant (Supplementary Figure S2D). Interestingly, CEY-4 protein levels appeared to increase upon demethylation (Supplementary Figure S2D and E), suggesting that the methylation status of its RG/RGG repeats may regulate CEY-4 protein levels.

CEY proteins are required for multiple aspects of germline development

The loss of YBPs in the germline has a major impact on the production and viability of progeny in other organisms (9,10,12). While *cey-1* and *cey-4* single mutants showed wild-type brood sizes, the loss of germline-specific CEY-2 or CEY-3 caused a significant reduction in progeny number (Supplementary Figure S3A). This defect was strongly exacerbated upon the loss of both CEY-2 and CEY-3 (Supplementary Figure S3B). By contrast, the loss of both CEY-1 and CEY-4 had little or no effect on brood size at either 20 or 25°C. Only at 26°C, an extreme growth temperature for *C. elegans*, was the sterility observed in *cey-1,-4* double mu-

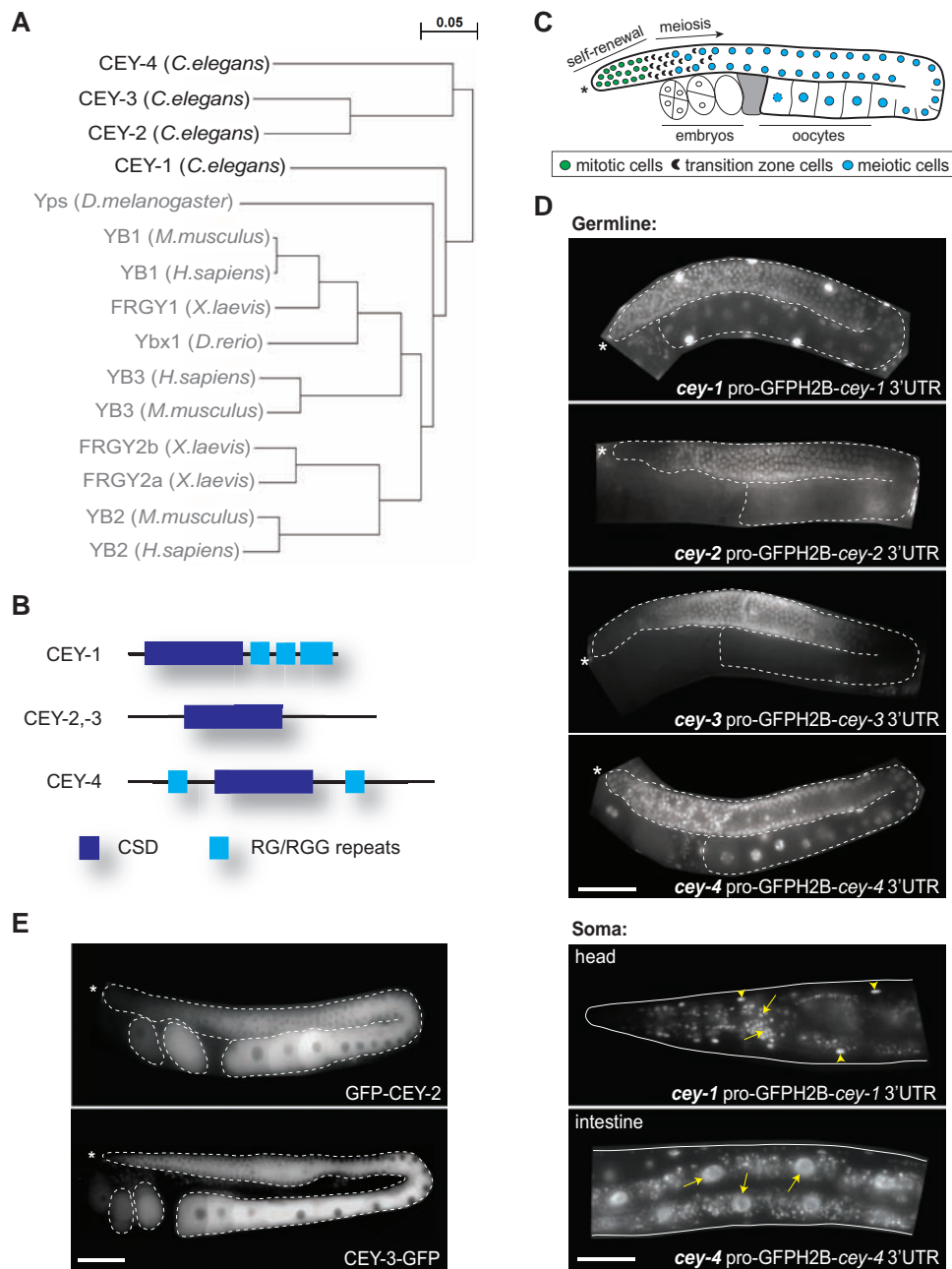


Figure 1. Characteristics of CEY proteins. (A) Phylogenetic tree showing a relation between CEYs and Y-box-binding proteins in other organisms, the closest being Yps in *Drosophila melanogaster*. The distance values show the number of amino acid substitutions as a proportion of the length of the alignment. (B) Besides the CSD, CEY-1 and CEY-4 contain RG/RGG repeats, which are absent in CEY-2 and CEY-3. (C) A schematic gonad with embryos. Self-renewing germ cells are located in the most distal part of the gonad. More proximally, germ cells enter meiosis via a so-called transition zone and, in adults, eventually differentiate into oocytes. Ovulated oocytes become fertilized by sperm stored in the spermatheca (in gray). Embryogenesis follows. (D) Fluorescent micrographs from live animals expressing histone reporter constructs for each of the four *cey* genes. The indicated *cey* promoters and the corresponding 3'UTRs drive expression of GFP fused to histone H2B (localizing GFP to the nucleus). The gonads are outlined by dotted lines and the animals by solid lines. Asterisks indicate the distal ends of the gonads. In the germline, *cey-1* and *cey-4* begin to be expressed in the distal most region of the gonad. In contrast, *cey-2* and *cey-3* are very lowly expressed distally but become strongly upregulated more proximally, when germ cells enter meiosis. In the soma, *cey-1* and *cey-4* are expressed in all tissues, albeit at different levels. Upper panel: *cey-1* reporter is expressed in neurons and muscles (yellow arrows point to exemplary neurons and yellow arrowheads to muscles). Lower panel: *cey-4* reporter is strongly expressed in the intestinal cells (yellow arrows). Scale bars = 50 μ m. (E) Fluorescent micrographs from live animals expressing GFP-tagged CEY-2 and CEY-3. Gonad and embryos are outlined by dotted lines. Consistently with the reporters shown above, both GFP-CEY-2 and CEY-3-GFP are upregulated upon the meiotic entry. The GFP signal starts to decrease in most proximal oocytes and disappears in early embryos. Scale bar = 50 μ m.

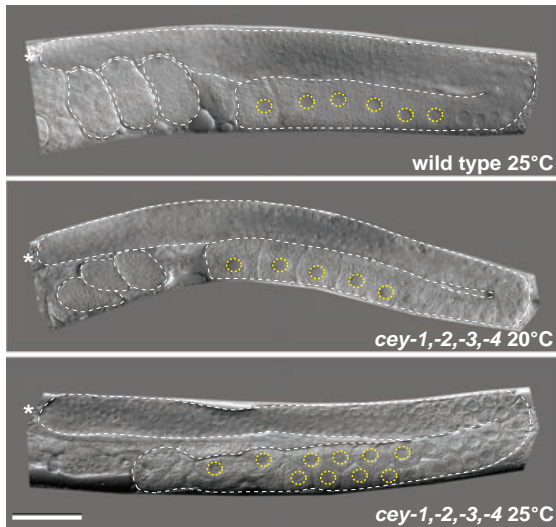


Figure 2. CEY proteins are essential for fertility. Light micrographs from live wild-type and mutant animals grown at the indicated temperatures. Gonads and embryos are outlined by white dotted lines, and oocyte nuclei by yellow dotted circles. Asterisk indicates the distal end of the gonad. Wild type looking oocytes form in the *cey-1,-2,-3,-4* quadruple mutant at 20°C, but all embryos fail to develop. A double row of smaller oocytes form in the *cey-1,-2,-3,-4* quadruple mutant at 25°C. Scale bar = 50 μ m.

tants (Supplementary Figure S3B). Finally, knocking out all four *cey* genes led to sterility, whereby the severity of the phenotype was strongly temperature-dependent, with more or less normal-looking oocytes at 20°C and a double row of smaller oocytes at 25°C (Figure 2). In summary, while CEY-1 and -4 have some function, CEY-2 and -3 appear to be the major CEY proteins in the germline.

Maintenance of stem cells and transit amplifying cells in the most distal part of the gonad, control of germ cell apoptosis and correct timing of oocyte maturation, are key events required for the production of healthy gametes. Focusing on the two germline-specific CEYs, CEY-2 and CEY-3, we wanted to evaluate a potential requirement for them in these processes. We first examined germ cell proliferation in animals subjected to *cey-2* and *cey-3* RNAi (*cey-2,-3* RNAi for brevity). To assess cell cycle progression, we used an antibody against Ser10-phosphorylated histone H3 (pH3), which stains condensed chromosomes marking cells in the M phase of the cell cycle. Animals depleted of CEY-2 and -3 had a significantly reduced number of proliferating cells in the distal gonad (Figure 3A) and, consistently, the mitotic zone was shorter in these gonads than in control wild-type gonads (Figure 3B). The length of the so-called transition zone, where germ cells enter into the meiotic prophase, remained similar between *cey-2,-3* RNAi and control animals (Figure 3C).

Next, we examined the effect of *cey-2,-3* knockdown on germ cell apoptosis in the mutant strain *ced-9(n1950)*. In this mutant, only the physiological apoptosis pathway is active, which removes defective germ cells and ensures oocyte quality (49). We observed a significant increase in the number of apoptotic cells in the RNAi-ed animals (Figure 3D). This could be due to increased rates of cell death or reduced rates of cell corpse clearance. To distinguish between these

two alternatives, we RNAi-ed *cey-2,-3* in the cell corpse engulfment-defective mutant *ced-1(e1735)*. We observed a significant increase in the number of germ cell corpses in the *ced-1(e1735); cey-2,-3* RNAi animals compared to mock-RNA-ied animals (Figure 3E), indicating that CEY-2 and -3 depleted animals have increased levels of germ cell apoptosis. Thus, CEY-2 and -3 are required for normal levels of germ cell proliferation and survival.

Finally, we examined the ability of oocytes to undergo normal oocyte maturation in CEY-2,-3 depleted animals. To monitor oocyte maturation, we used two phosphorylation-specific markers; one for the mitogen-activated protein kinase 1 (MPK-1) and one for Aurora B kinase (AIR-2). In wild-type gonads, these markers highlight the most proximal oocytes (so-called -1 and -2 oocytes). In contrast, depleting CEY-2,-3 resulted in the appearance of these markers in more distal oocytes (Figure 3F and G), suggesting premature maturation.

CEYs are essential components of germline mRNPs

A major function of YBPs in the germline is to bind and package mRNAs into mRNPs for cytoplasmic storage (8,50). To look at the association between CEYs and mRNAs globally, we isolated RNA following FLAG IPs performed on extracts of animals expressing FLAG-tagged versions for CEY-1, CEY-2 and CEY-4. MYC IPs performed on the same extracts served as controls. The different replicates correlated with each other very well (Supplementary Figure S4A), indicating high reproducibility. Comparing the FLAG IP data to the respective MYC control IPs revealed no striking enrichment of specific mRNAs (Supplementary Figure S4B-D). We thus conclude that CEYs do not have a clear preference for binding specific subsets of mRNAs, a result expected for proteins that either do not bind mRNA or interact with messages in an unspecific fashion. As YBPs from other model organisms often interact more generally with mRNA, we believe that this is also the case in *C. elegans*. Curiously, we found that many mRNAs were depleted in the case of all three FLAG IPs compared to MYC control IPs (Supplementary Figure S4B-D). This was most strongly apparent for the germline-specific CEY-2 (Supplementary Figure S4C). We speculated that the observed depletion of mRNAs might stem from varying expression of a given CEY protein in different tissues. To test this, we selected the mRNAs 'depleted' from FLAG-CEY-2 IPs and monitored their expression in the soma versus the gonad (Supplementary Figure S4E-F). As predicted, these mRNAs were predominantly expressed in the soma, a tissue in which the germline-specific CEY-2 is not present.

Two previous studies had shown that both the conserved RNA helicase CGH-1/DDX6 and the STAR-domain RNA-binding protein (RBP), GLD-1/Quaking, interact with CEYs via RNA (14,29). In a reverse immunoprecipitation experiment, we purified FLAG-tagged CEY-1 and CEY-4 in the presence or absence of RNase. The samples were then examined by MS analysis to obtain a global view of RNA-dependent and RNA-independent protein interactions. We found that CGH-1 and GLD-1 co-purified with CEYs in an RNA-dependent fashion (Supplementary Table S2–3 and Figure S5 and 6, green squares). These data

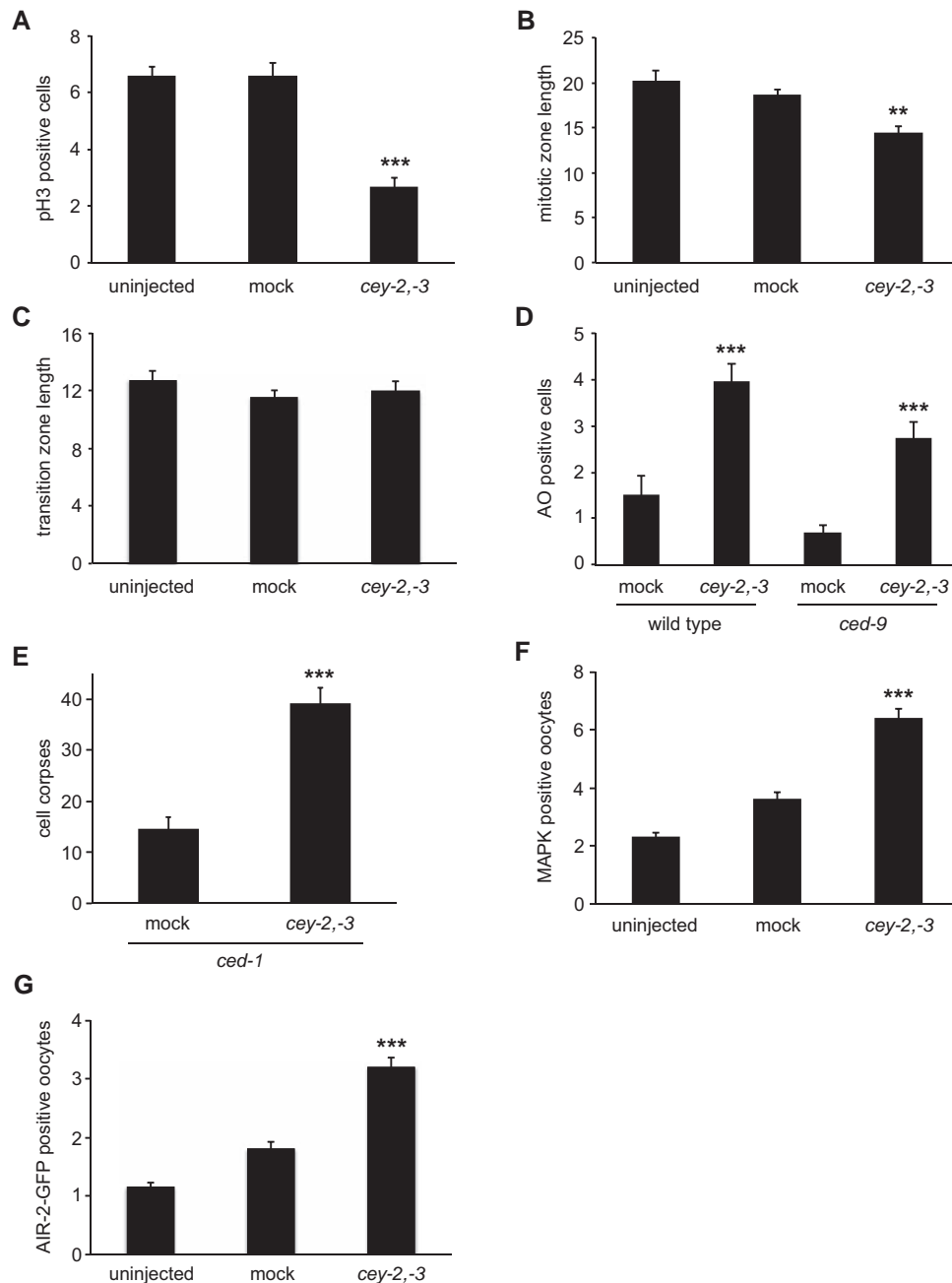


Figure 3. Germline defects in the absence of CEY proteins. Gonads were either not injected (uninjected), control injected (mock RNAi) or injected with RNAi clones targeting both *cey-2* and *cey-3* (*cey-2,-3* RNAi). (A–G) Error bars represent SEM. Asterisks denote *P*-values <0.01 by *t*-test. (A) Proliferative germ cells were stained with anti-pH3 antibody and the number of positive cells was subsequently quantified by fluorescence microscopy. (B) The proliferative zone was shorter in *cey-2,-3* RNAi gonads compared to controls, while the length of the transition zone remained constant (C). (D) Depletion of CEY-2,-3 caused an increase of acridine orange (AO) stained apoptotic cells in both wild-type and *ced-9(n1950)* animals. (E) RNAi of *cey-2,-3* in the cell corpse engulfment-defective strain, *ced-1(e1735)*, resulted in a significant increase in the number of germline corpses. (F and G) RNAi of *cey-2,-3* resulted in premature appearance of activated MAPK in proximal oocytes and AIR-2-GFP on the chromosomes of oocytes in diakinesis.

were confirmed by co-IPs performed again with or without RNase treatment on FLAG-CEY-2 (chosen instead of FLAG-CEY-1 to include a germline-specific CEY protein) and FLAG-CEY-4, and detecting specific proteins by western blot (Figure 4A). Intriguingly, while RNase treatment led to the loss of the interaction between CEYs and several germline RBPs, we observed that the interaction with multi-

ple ribosomal proteins was maintained (Supplementary Table S2–3, Figure S5 and 6, red dots), suggesting a potential direct link between CEYs and ribosomes.

The absence of CGH-1 causes the accumulation of aberrant RNP granules, which have been proposed to represent an aggregation of abnormal mRNPs (16–19). Indeed, knockdown of *cgh-1* also resulted in the localization of

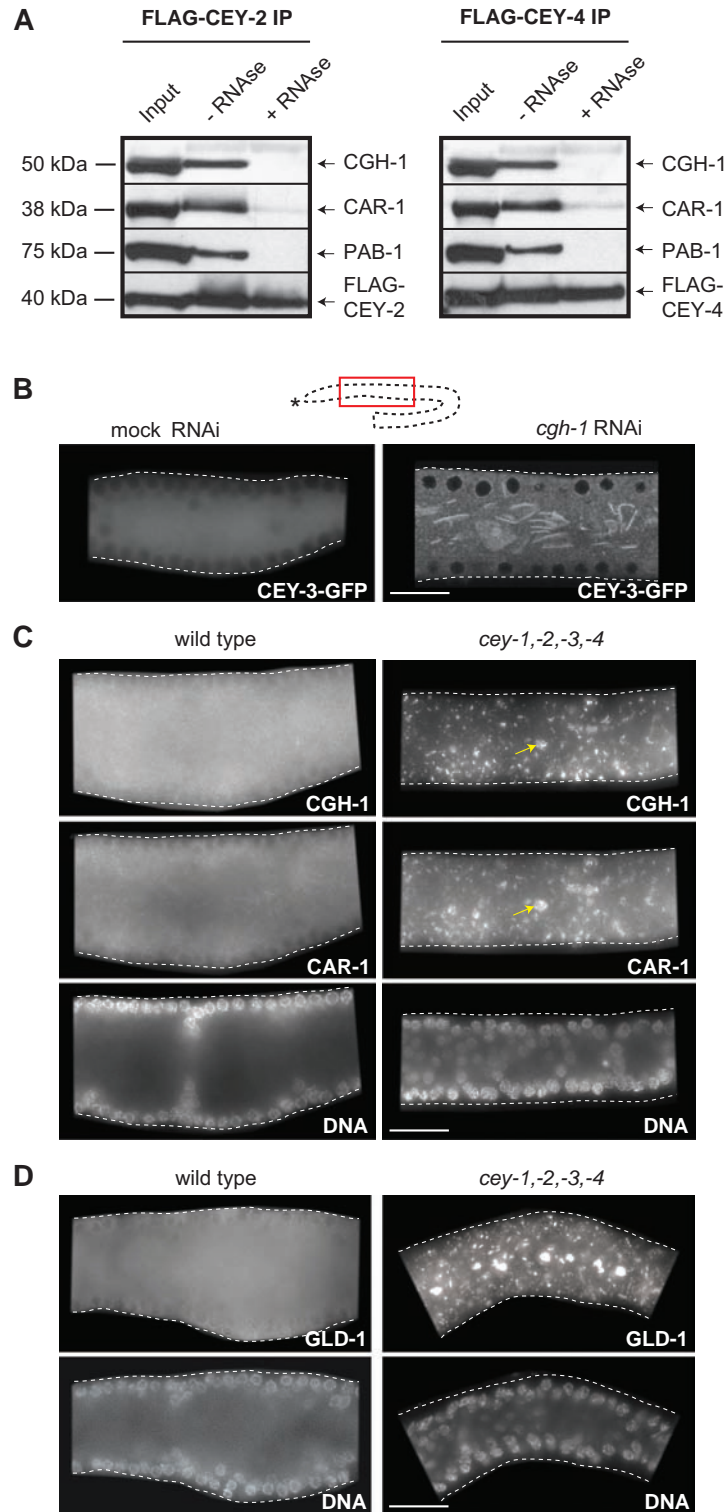


Figure 4. CEYs are required for the integrity of germline mRNPs. (A) FLAG IPs performed in the presence or absence of RNase on extracts from transgenic animals expressing either FLAG-CEY-2 or FLAG-CEY-4. In both cases, CGH-1, CAR-1 and PAB-1 were no longer co-IPed upon RNase treatment. (B–D) All shown images come from the medial gonadal region, boxed in red on the schematic gonad. All partial gonads are outlined by dotted lines. Asterisk indicates the distal end of the gonad. (B) Fluorescent micrographs of medial gonads from live animals expressing CEY-3-GFP. In the cytoplasm of wild-type gonads, the CEY-3-GFP was distributed evenly. Upon *cgh-1* RNAi, CEY-3-GFP localized to sheet-like structures. Scale bar = 20 μ m. (C) Fluorescent micrographs of wild-type and *cey-1,-2,-3,-4* mutant gonads co-immunostained for CAR-1 and CGH-1, and additionally stained with DAPI to visualize DNA. Both proteins localized to aberrant RNP granules in *cey* mutant germlines (yellow arrow points to an exemplary RNP granule). Scale bar = 20 μ m. (D) Fluorescent micrographs of wild-type and *cey-1,-2,-3,-4* mutant gonads immunostained for GLD-1 and stained with DAPI. GLD-1 also localized to aberrant granules in the absence of CEY proteins. Scale bar = 20 μ m.

GFP-tagged CEY-3 to abnormal granules in the cytoplasmic core of the gonad (Figure 4B). To test if CEYs play a role in RNP regulation, we stained CEY(-) gonads for both CGH-1 and CAR-1/Rap55, a conserved RBP that is usually present on CGH-1-bound mRNAs (14). Indeed, both factors localized to aberrant RNP granules in the *cey-1*; *cey-2 cey-3*; *cey-4* (for brevity *cey-1,-2,-3,-4*) quadruple mutant (Figure 4C). Furthermore, we found that GLD-1 was also present in aberrant RNPs (Figure 4D). Thus, CEYs are important for normal RNP appearance in the *C. elegans* germline, as their homologs are in other organisms.

CEY-1 and CEY-4 are required for the formation of large polysomes in the soma

Besides germline defects, the loss of YBPs can impact somatic development. For example, YB-1 depleted mice are embryonic lethal (51), though it remains possible that this lethality may reflect a maternal function of YB-1. Initially, we observed that the *cey-1(ok1805)* mutant grew significantly slower than wild-type at 20°C. However, we found that the *ok1805* mutation, thought to be a null, gave rise to a truncated protein that contained both RNA-binding motifs (RNP1 and RNP2) of the CSD (data not shown) (2,23), and might therefore still bind RNA. To create a functional null, we generated a new *cey-1* mutation (*rrr12*), using the CRISPR/Cas9-system (24). We used this mutant in subsequent studies. We found that *cey-1(rrr12)* mutants, thereafter referred to simply as *cey-1*, no longer displayed the growth delay observed in *cey-1(ok1805)* mutants. This might suggest a slight dominant-negative effect of the truncated CEY-1 protein encoded by the *cey-1(ok1805)* mutant. Also the *cey-1,-4* double mutant had no apparent developmental defects compared to wild-type under normal growth conditions. Furthermore, apart from the sterile phenotype observed at 26°C, the *cey-1,-4* mutant showed no defects in its response to different stress cues, such as low or high temperature or food deprivation. The same was true for longevity (data not shown). Similarly, neither the two single mutants (*cey-1* and *cey-4*) nor the double mutant (*cey-1,-4*) showed any significant irregularities in diacetyl chemotaxis (Supplementary Figure S7), despite the fact that CEY-1 was strongly expressed in neurons (Figure 1D).

YBPs can act as translational repressors (4,6,7). For this reason, we monitored mRNA translation by polysome profiling. In this approach, ‘ribosomal’ fractions harbor ribosomes actively engaged in translation (Supplementary Figure S8A). While the depletion of the germline-specific CEY-2 and -3 caused no obvious change in the distribution of ribosomes (Figure 5A), the removal of CEY-1 and -4 resulted in a striking loss of large polysomes (multiple ribosomes associated with mRNAs) with a concomitant increase in monosomes and disomes (Figure 5B). This was very surprising, considering the absence of any obvious phenotype in the *cey-1,-4* mutant. Polysome profiles of heat-shocked animals (Supplementary Figure S8B and C), suggested that the effect observed in *cey-1,-4* mutants did not reflect a stress response. Furthermore, the *cey-1,-4* mutant responded to the heat stress as wild-type animals did, namely, by reducing translating ribosomes, consistent with

our previous observation that these mutants deal with stress as well as wild-type animals.

As most cells in adult *C. elegans* are germ cells, we performed polysome profiling also on germline-less *glp-4* mutants to find out what contribution the germline has on the polysome profile. Strikingly, we found that virtually all subpolysomal (repressed or poorly translated) mRNAs were germline specific (disappeared in the *glp-4* mutant background) (Supplementary Figure S8D and E). Thus, it seemed unlikely that the loss of polysomes in *cey* mutants was caused by germline defects. To test this directly, we crossed the *cey-1,-4* mutant into another temperature-dependent germline-less mutant, *glp-1(e2144)*. In these animals, we still observed the loss of large polysomes and, additionally, some intermediate ribosomal peaks (Figure 5C). Because CEY-4 expressed specifically in the germline and CEY-2 expressed from the *cey-1* promoter both failed to rescue the polysome defect (Figure 5D and E and Supplementary Figure S8F and G), we conclude that, in general, accumulation of large polysomes depends on the somatic CEY proteins. Interestingly, by monitoring a FLAG-tagged version of CEY-1 and the endogenous CEY-4, we found that the distribution of CEY-1 and CEY-4 between sub- and polysomal fractions from wild-type animals was not identical. While CEY-4 was present in both sub- and polysomal fractions, potentially indicating an interaction with ribosomes, CEY-1 was mainly present in the submonosomal fractions (Figure 5F). Consistent with nonidentical distributions along the gradient, the polysome profiles of individual *cey-1* and *cey-4* single mutants did not match. The *cey-4* single mutant showed a drop in larger polysomes and an increase in mono- and disomes, similar to the *cey-1,-4* double mutant, albeit to a lesser extent (Supplementary Figure S8H). The *cey-1* single mutant, on the other hand, showed only a slight decrease of large polysomes without affecting mono- or disomes (Supplementary Figure S8I). Thus, CEY-1 and -4 may have specific functions, though the fact that the loss of CEY-1 further increases both the loss of large polysomes and the accumulation of mono- and disomes in *cey-4* single mutants, suggests that there is some degree of redundancy between CEY-1 and CEY-4.

CEY-1 and -4 appear dispensable for normal levels of protein synthesis

Considering the importance attributed to polysomes in maintaining high translation rates, we were surprised to see that the *cey-1,-4* double mutant grew similar to wild-type. To assess global protein synthesis rates in these animals, we used SURface SENSing of Translation (SUNSET) (34). SUNSET is based on the incorporation of puromycin into newly synthesized peptides and the subsequent detection of the incorporated puromycin by western blotting using a specific monoclonal antibody. Consistent with the normal growth of *cey-1,-4* mutants, we detected no obvious decrease in puromycin incorporation (Figure 6A), suggesting that, on the global scale, there is no major change in the translation rates in *cey-1,-4* mutants. To confirm this, we additionally performed the ³⁵S-Met labeling assay (35). The results were consistent with the data obtained from the SUNSET experiment (Figure 6B). In agreement with those findings, the to-

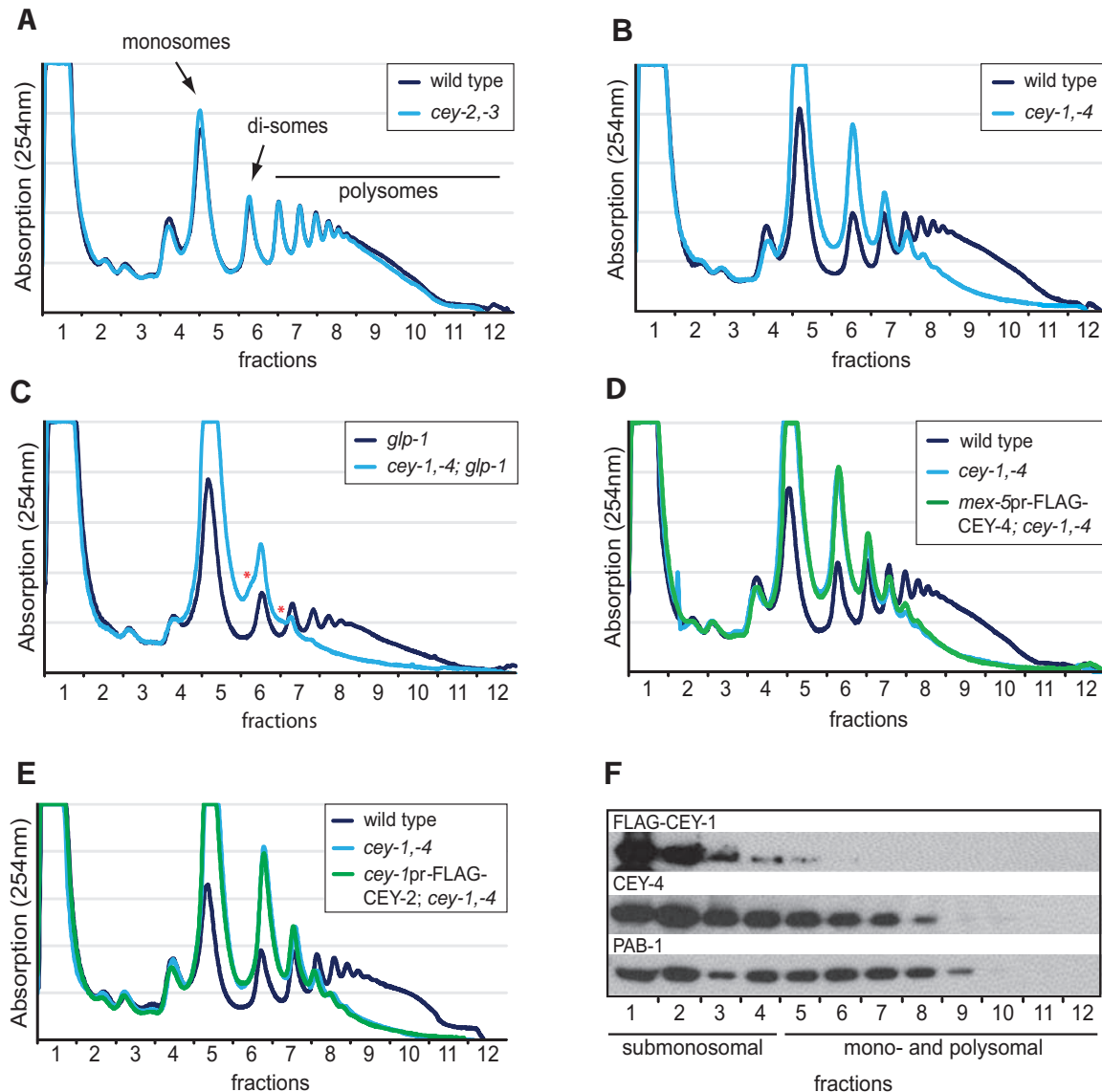


Figure 5. CEY-1 and CEY-4 are essential for the assembly of large polysomes. (A) Polysome profiles from wild-type and *cey-2,-3* mutants were indistinguishable. Indicated are the positions of mono-, di- and polysomes. (B) The depletion of CEY-1 and CEY-4 caused a strong decrease of large polysomes with a concomitant increase of mono- and disomes. (C) The loss of polysomes observed in *cey-1,-4* mutants was also observed in the germline-less *glp-1* (*e2144*) background. Red asterisks indicate the positions of additional small peaks present to the lighter side of normal di- and trisome peaks. (D) A FLAG-tagged CEY-4 transgene (FLAG-CEY-4) expressed specifically in the germline from the *mex-5* promoter could not restore polysomes in the *cey-1,-4* mutant. The same fusion protein when expressed ubiquitously, partially restored polysomes (see Supplementary Figure S8F). (E) Expressing a FLAG-tagged CEY-2 transgene (FLAG-CEY-2) from the *cey-1* promoter also did not restore polysomes in the *cey-1,-4* mutant. Expression of a FLAG-tagged CEY-1 transgene (FLAG-CEY-1) from the *cey-1* promoter partially restored polysomes (see Supplementary Figure S8G). (F) Proteins were extracted from each of the 12 fractions from a polysome profiling experiment and analysed by western blot. CEY-1 (FLAG-tagged) was mainly present in subpolysomal fractions, while a significant part of CEY-4 was additionally found in ribosomal fractions. PAB-1 was, as expected, present in both submonosomal and ribosomal (mono- and polysomal) fractions and served here as a control.

tal amounts of protein were similar between wild-type and the *cey-1,-4* mutant (Supplementary Figure S9A).

The global loss of large polysomes in *cey-1,-4* mutants suggested that there could be less ribosomes per specific mRNAs in the mutant compared to wild-type. A recent study in human cells showed that a decrease in ribosome number activates the elongation machinery via a controlled feedback loop (52). The amount of translation-inhibiting EEF-2 kinase (*eef-2k*) decreases, thereby reduc-

ing the amount of phosphorylated EEF-2, the inactive form of this essential elongation factor. This might allow fewer ribosomes to translate more efficiently, producing the same protein output as in wild-type. In the *cey-1,-4* mutant, however, we found that both *efk-1* (*C. elegans* homolog of *eef-2k*) mRNA levels (data not shown) as well as the EEF-2 phosphorylation status remained unchanged compared to wild-type (Supplementary Figure S9B), suggesting that the

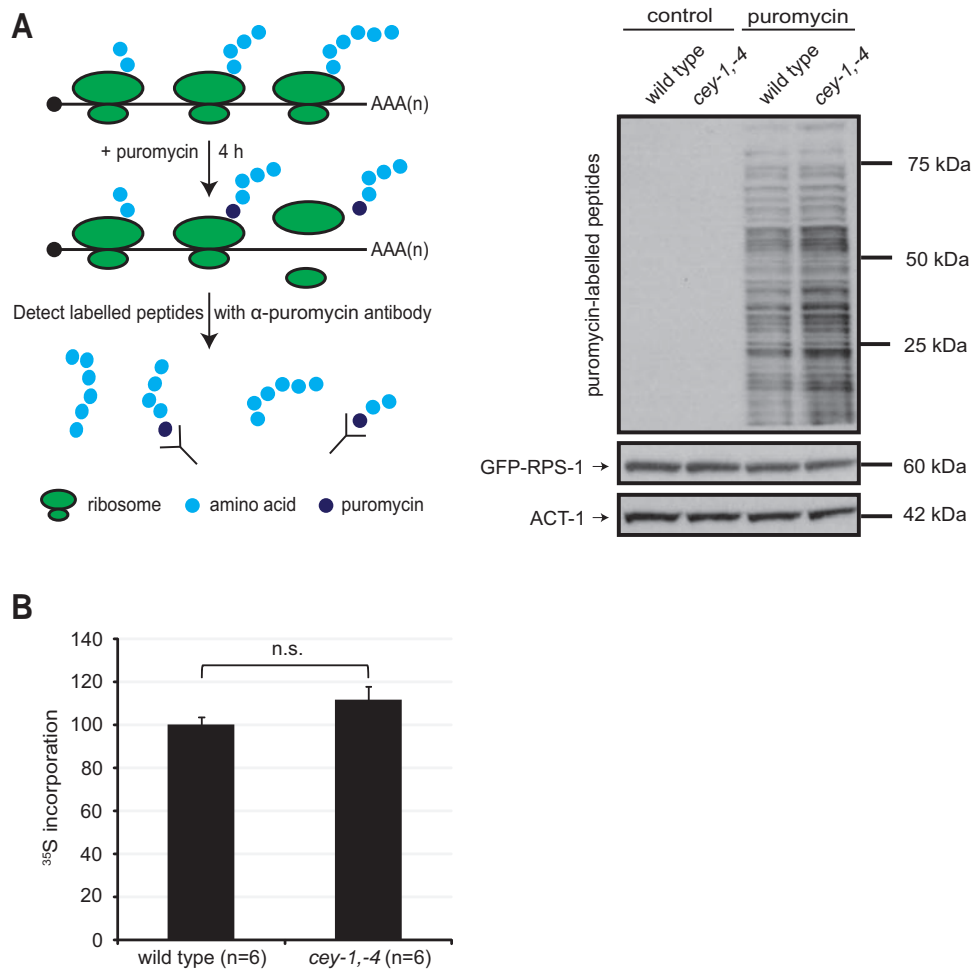


Figure 6. Global protein synthesis rates are similar between wild-type and *cey-1,-4* mutants. (A) Surface Sensing of Translation (SuNSET) was adapted for *Caenorhabditis elegans*. Animals were grown with or without puromycin. A 4-h treatment was sufficient to detect puromycin incorporation into nascent proteins on a western blot, but, importantly, did not yet affect global translation (data not shown). Actin (ACT-1) was used as a loading control. Additionally, as an external loading control, extracts were spiked with an identical amount of extract from animals expressing GFP-tagged RPS-1, which were grown without puromycin. (B) Animals were grown in ^{35}S -methionine-labeled OP50 bacteria for 3 h, and the amount of radioactivity incorporated into newly synthesized proteins was measured for wild-type and *cey-1,-4* mutants. The wild-type value was set to 100.

above-mentioned feedback mechanism is unlikely to compensate for the loss of polysomes.

CEY proteins are broadly required for mRNA accumulation

To obtain a more detailed view of mRNA levels and translation in *cey-1,-4* mutants, we performed ribosome profiling combined with total RNA sequencing (53); these data may reveal relative changes of mRNA levels and translation within a given sample but cannot be used to compare absolute mRNA levels between different samples. The replicates correlated very well with one another for both the ribosome profiling experiment as well as for the total RNA sequencing (Supplementary Figure S10), indicating high reproducibility. We first created start- and stop codon profiles of the 5' ends of all ribosome-protected fragments (RPFs), but found no apparent differences between profiles from wild-type and *cey-1,-4* mutants (Supplementary Figure S11). Interestingly, we observed a gradual increase of reads along mRNA in both wild-type and mutant animals

(Supplementary Figure S11), suggesting that the speed of translation elongation gradually decreases toward the end of messages in *C. elegans*. This could help, for example, in co-translational protein folding that might become more problematic with increased polypeptide length (54).

To determine the impact of CEY-1 and -4 on mRNA levels and translation, we globally compared the changes on the mRNA level to those on the RPF level in a scatter plot. We observed a group of transcripts that showed relatively small changes in mRNA abundance but displayed a pronounced reduction of RPFs (Figure 7A, red arrow). We found that the majority of the messages that were downregulated predominantly at the RPF level were germline-specific (Figure 7B and Supplementary Figure S12A and B). As germline mRNAs tend to be poorly translated, we also observed that messages normally depleted from ribosomal fractions were downregulated at the RPF level (Figure 7C and Supplementary Figure S12C). Interestingly, many of these CEY-1 and -4 regulated germline mRNAs encode fac-

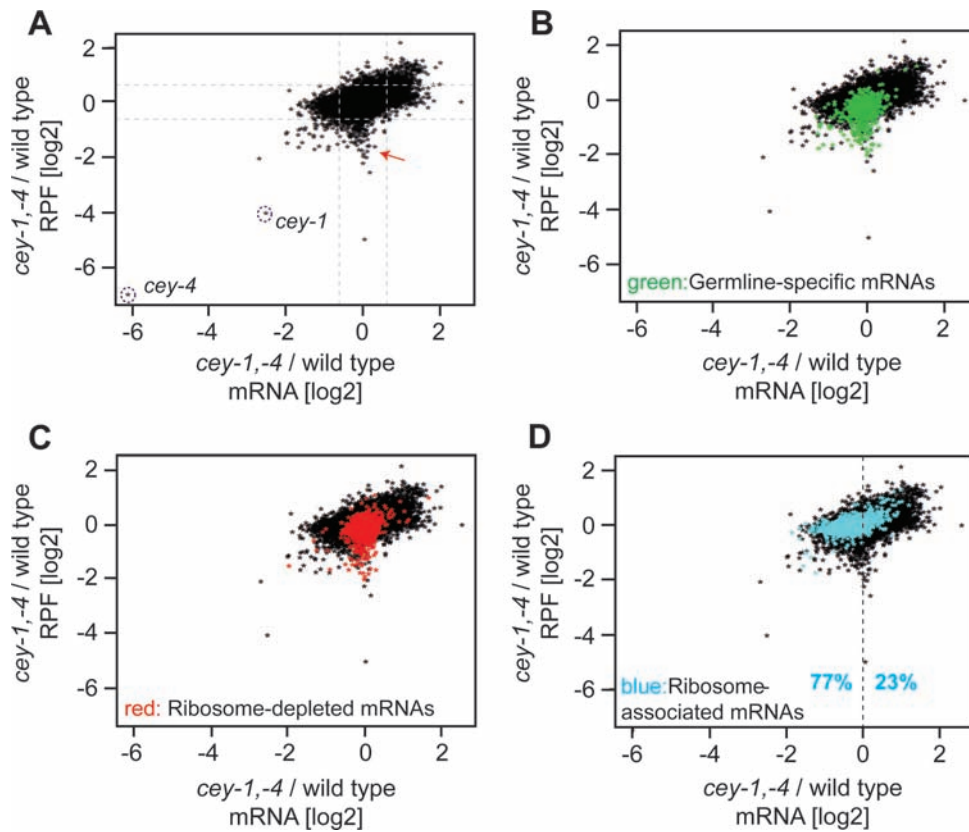


Figure 7. CEY-1 and CEY-4 regulate mRNA translation and abundance. Both ribosome profiling and total RNA sequencing were performed in duplicates. The mean values were calculated and the wild-type values were subtracted from the *cey-1,-4* values. The changes in mRNA levels were then plotted against the changes in RPF levels (indicating translation). The same plot is shown in A–D. The ‘germline-specific mRNAs’, ‘ribosome-depleted mRNAs’ and ‘ribosome-associated mRNAs’ (marked in B, C and D, respectively) were selected as shown in Supplementary Figure S12A–C and G and H. (A) Gray dotted lines demarcate 1.5-fold changes. As expected, *cey-1* and *cey-4* reads were strongly depleted in the mutants. (A) Gray dotted transcripts (red arrow) displayed little or no change in mRNA levels but showed reduced association with ribosomes. (B) In green are marked mRNAs expressed in gonads (mostly germline mRNAs) but not in the soma (see Supplementary Figure S12A and B). (C) In red are marked mRNAs that are depleted from mono- and polysomes (i.e. are either poorly translated or repressed) in wild-type animals (see Supplementary Figure S12C). (D) In blue are marked mRNAs enriched in mono- and polysomes in wild-type animals (see Supplementary Figure S12G and H). The vertical dotted line marks no change at the mRNA level in wild-type and mutant. The majority of ‘ribosome-associated mRNAs’ (77%) appear to the left of the dotted line. Therefore, compared to all mRNAs, genes in this subset have a higher chance to be lower in abundance in the mutant (P -value $< 2.2 \times 10^{-16}$ by t -test).

tors important for the oocyte-to-embryo transition, such as RME-2, EGG-1,-2,-4,-5 and OMA-2 (Supplementary Figure S12D–F and Supplementary Table S4). Thus, reduced translation of these messages may be responsible for the fertility defects observed in *cey-1,-4* mutants at restrictive temperature (Supplementary Figure S3B). In stark contrast, we found that messages normally enriched in ribosomal fractions (translated) (Supplementary Figure S12G and H) showed, in general, a decrease in mRNA abundance in the mutants (Figure 7D). We performed a series of qRT-PCR experiments to validate these global observations. Indeed, the abundance of ‘ribosome-associated mRNAs’ (mainly ubiquitous or soma-specific mRNAs) was in most cases strongly reduced in the absence of CEY-1 and -4 (Figure 8A), but remained constant in *cey-2,-3* mutant animals (Figure 8A). We also found that germline-specific mRNAs were more strongly affected in *cey-2,-3* than in *cey-1,-4* mutants (Figure 8B), which is consistent with a predominant role for CEY-2 and -3 in the germline. Nevertheless, the absence of all four CEY proteins further reduced mRNA levels (Figure 8B). As expected, this reduction in

mRNA abundance had a major effect on protein accumulation in the germline, as exemplified by RME-2 (Figure 8C). Finally, as RPF levels of oocyte-to-embryo transition factors decreased more strongly compared to mRNA levels (Supplementary Figure S12D–F and Supplementary Table S4), we looked for potential redistribution of these messages from mono- and polysomal fractions to submonosomal fractions in the *cey-1,-4* mutant (Supplementary Figure S13A). Indeed, we observed a redistribution of *rme-2*, but not of *oma-2* or *egg-1* (Supplementary Figure S13B). It is possible that these messages shift predominantly from heavier to lighter polysomes. However, as mRNAs of oocyte-to-embryo transition regulators are generally present at low levels in polysomal fractions, detecting such redistributions may be difficult.

DISCUSSION

The conserved requirement for CEY proteins in the germline

All four CEYs are expressed in the germline. However, whereas CEY-1 and -4 are present in the self-renewing germ

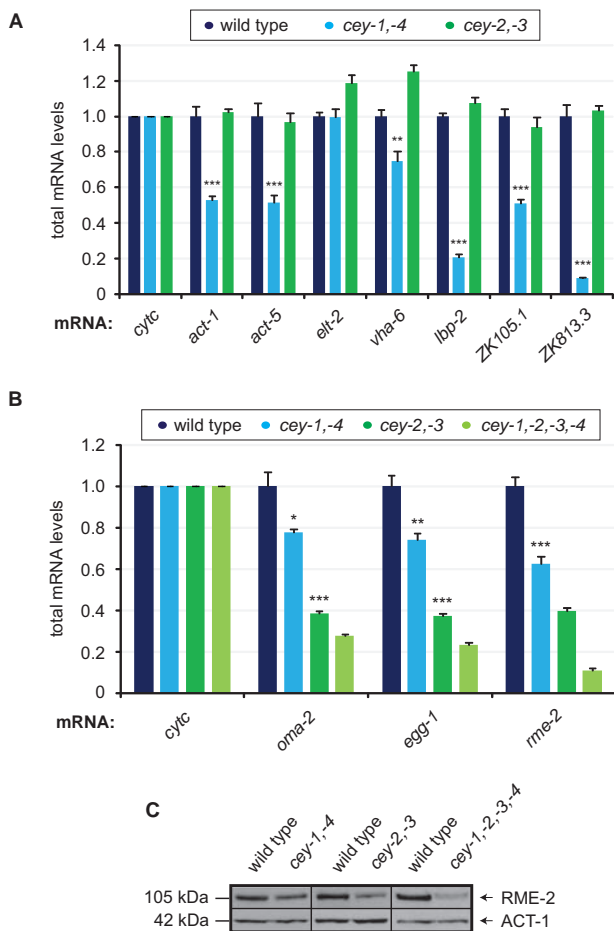


Figure 8. CEYs promote mRNA abundance in the soma and the germline. (A and B) Polysome profiling was performed for wild-type, *cey-1,-4*, *cey-2,-3*, and *cey-1,-2,-3,-4* animals. qRT-PCR analysis was performed on RNA extracted from pooled sucrose fractions 1–12 (total RNA) (see Supplementary Figure S13A). The data were normalized to a mouse mRNA, *cytc* (cytochrome c), to correct for any discrepancies during RNA extraction and cDNA synthesis. One asterisk denotes P -value < 0.05 by t -test. Two asterisks denote P -value < 0.01 by t -test. Three asterisks denote P -value < 0.005 by t -test. Error bars represent SEM. (A) The abundance of tested ubiquitous (expressed in germline and soma) or soma-specific mRNAs was reduced in the *cey-1,-4* mutant but not in the absence of the germline-specific CEY-2 and -3. (B) The abundance of germline-specific transcripts was more strongly affected in the *cey-2,-3* double mutant compared to *cey-1,-4* mutant animals. The mRNA levels dropped even further in the *cey-1,-2,-3,-4* quadruple mutant. (C) Changes in RME-2 protein levels mirrored the changes of mRNA levels (B), showing the strongest decrease in the *cey-1,-2,-3,-4* mutant.

cell compartment in the most distal gonad, the most likely redundant CEY-2 and CEY-3 are only weakly expressed in this gonadal region. They become strongly upregulated more proximally, i.e. upon the entry into meiosis. Our observations that the *cey-2,-3* mutant animals produce only around half of wild-type progeny, while the *cey-1,-4* double mutants have less progeny only when challenged with extreme temperature, suggest that CEY-2 and -3 are the predominant CEY proteins in the germline. We speculate that they are induced to support CEY-1 and -4 to cope with the bulk of newly synthesized maternal mRNAs, which are then transported with general cytoplasmic flow into grow-

ing oocytes (55). Consistent with this idea, CEY-2 and -3 disappear in early embryos, coincidentally with the degradation of most maternal mRNAs (56,57). Indeed, abundance of tested maternal mRNAs was more strongly affected in *cey-2,-3* mutant animals, compared to *cey-1,-4* double mutants, supporting a predominant role for CEY-2 and -3 during oogenesis. Essential RBPs and germline RNP components, such as GLD-1, CGH-1 and CAR-1, are also strongly upregulated when germ cells enter meiosis (14,15,58) and interact, via RNA, with CEYs (14,29), suggesting that all these proteins are present in the same RNPs during oogenesis. The observation that both the *cgh-1* mutant (15) and the *cey-1,-2,-3,-4* mutant display similar germline defects, such as reduced germ cell proliferation, enhanced apoptosis and defective oocytes, supports a functional connection between these proteins. Even though the aberrant RNP granules observed in *cey-1,-2,-3,-4* gonads appear distinct from the solid square sheets found in the absence of *cgh-1* (16–19), the formation of abnormal aggregates is likely to impact the regulation of germline messages. Although the connection between large RNP formation and function in mRNA regulation remains unclear, we found that the abundance of maternal mRNAs was strongly affected in the absence of CEYs. We therefore believe that CEY proteins play an important role in the binding and stabilization of maternal messages during oogenesis, similar to what has been postulated for mouse and *Xenopus* YBPs (6–10). This may involve the formation, maintenance and/or disassembly of functional RNP granules to guarantee correct spatial and temporal mRNA translation.

A function of CEY proteins in the accumulation of large polysomes

In contrast to the expected results in the germline, we found that the loss of CEY proteins in the soma causes a striking reduction of large polysomes, with a simultaneous increase in monosomes and disomes. Our ribosome profiling data combined with mRNA sequencing and subsequent qRT-PCR validation suggest that the abundance of messages normally enriched in the polysomes decreases. One possibility, therefore, is that CEY proteins are also required for mRNA stability in the soma, consequently permitting accumulation of more ribosomes on mRNAs and thus allowing the formation of larger polysomes. In this scenario, CEYs might promote mRNA stability via direct association with mRNAs and, by doing so, protect mRNAs from destabilizing factors such as deadenylases or de-capping enzymes. We attempted to test the stability of specific mRNAs in *cey* mutant adults by inhibiting Pol II-mediated transcription and monitoring mRNA decay. However, although several drugs inhibited Pol II transcription, they also interfered with the expression of ribosomal RNAs and, consequently, with translation, rendering these experiments inconclusive.

Interestingly, the germline-specific protein CEY-2, when expressed in the soma from the *cey-1* promoter, was not able to rescue the polysome defect observed in the *cey-1,-4* mutant. This suggests that, to some extent, CEY-1 and -4 have different functions than CEY-2 and -3, which might be related to their potential association with the ribosome. This idea is based on the immunoprecipitation results, which

suggest that CEY-1 and CEY-4 might directly interact with ribosomal proteins. Other proteins have been shown to bind and potentially regulate ribosomes. For example, nucleolin binds ribosomal proteins via its RG/RGG motifs (59). Whether this represents a broader role of the RG/RGG motifs in ribosomal interactions remains unknown, but it is intriguing that the human genome encodes over 1000 proteins with at least one RG/RGG repeat, in most cases with unknown molecular functions (47). Similarly, the two somatic nematode CEY proteins also have RG/RGG repeats that can be di-methylated. A potential role of this methylation in polysome accumulation seems unlikely, as we found that polysomes were normally present in *prmt-1* mutants (our unpublished observation). However, this does not exclude the possible role of the RG/RGG repeats of CEYs in regulating some aspect of ribosome biology, which could have an impact on efficient translation and/or mRNA stability. Testing this will require mutating the RG/RGG motifs in otherwise rescuing proteins and is an interesting objective for the future research. Intriguingly, in addition to the loss of large polysomes in *cey-1,-4* mutants, we observed the accumulation of potentially partial or aberrant ribosomes. Partial ribosomal peaks have been described previously. However, these were found on the heavier side of ribosomes and were shown to represent so-called ‘half-mers’ (60–62). They form due to problems in 60S binding or availability and represent a 40S subunit bound to mRNA. In contrast, the unusual ‘peaks’ in *cey* mutants accumulate to the lighter side of ribosomes (observed for di- and trisomes). The formation of potentially abnormal ribosomes suggests that the overall number of ‘healthy’ ribosomes might be lower in *cey* mutant animals. However, the causal relation between the appearance of these, potentially abnormal, ribosomes and the loss of large polysomes remains to be determined.

The biological (in)significance of *C. elegans* polysomes

Our most striking finding is that the apparent loss of large polysomes in *cey-1,-4* mutants appears to have little or no negative impact on global translation rates. This stands in stark contrast with the general view that large polysomes contribute significantly to overall protein production. Puromycin release assays showed that large polysomes are indeed engaged in translation in *C. elegans*. So, in the absence of polysomes, how can protein synthesis rates remain at wild-type levels? One possible explanation is that an enhanced speed of translation elongation might compensate for the loss of polysomes. If we assume that the number of functional ribosomes is reduced in *cey-1,-4* mutant animals, maintaining wild-type EEF-2 levels means that the ratio of available elongation machinery factors per ribosome may increase, possibly providing a ‘passive’ way to make translation elongation more efficient. However, testing this hypothesis will require developing methodology to measure the speed of elongation in *C. elegans*, which is currently not feasible. Independent of whether elongation speed is affected or not, our study has raised a fundamental question: what is the accumulation of multiple ribosomes on messages required for? A regulatory function appeared to us most likely. However, under several different stress

conditions, the *cey-1,-4* mutant performed as well as wild-type did. Nevertheless, it remains possible that a potential disadvantage of the mutant might only become apparent in nonlaboratory conditions, where slight defects could have a large impact on the overall fitness.

ACCESSION NUMBERS

The NGS data has been uploaded to the GEO database (accession number is GSE62861).

SUPPLEMENTARY DATA

Supplementary Data are available at NAR Online.

ACKNOWLEDGEMENTS

We thank Witek Filipowicz, Raúl Méndez and Jan Seebacher for discussions. We would also like to thank everyone from the genomics facility at the Friedrich Miescher Institute for library preparation and deep sequencing. Some of the strains were provided by the Caenorhabditis Genetics Center (CGC) funded by the NIH. The *cey-3(tm2839)* mutant was provided by the Mitani lab through the National Bio-Resource Project of the MEXT, Japan.

FUNDING

Swiss National Science Foundation [31003A_149402 to R.C.], Novartis Research Foundation to Friedrich Miescher Institute for Biomedical Research. National Health and Medical Research Council [APP606575, APP1042848 to P.R.B.], Australian Postgraduate Awards (APA) scholarship [to M.R.]. Funding for open access charge: Friedrich Miescher Institute for Biomedical Research.

Conflict of interest statement. None declared.

REFERENCES

- Sommerville, J. (1999) Activities of cold-shock domain proteins in translation control. *Bioessays*, **21**, 319–325.
- Landsman, D. (1992) RNP-1, an RNA-binding motif is conserved in the DNA-binding cold shock domain. *Nucleic Acids Res.*, **20**, 2861–2864.
- Sasaki, K. and Imai, R. (2012) Pleiotropic roles of cold shock domain proteins in plants. *Front. Plant Sci.*, **2**, 116.
- Eliseeva, I.A., Kim, E.R., Guryanov, S.G., Ovchinnikov, L.P. and Lyabin, D.N. (2011) Y-box-binding protein 1 (YB-1) and its functions. *Biochemistry (Moscow)*, **76**, 1402–1433.
- Ruzanov, P.V., Evdokimova, V.M., Korneeva, N.L., Hershey, J.W. and Ovchinnikov, L.P. (1999) Interaction of the universal mRNA-binding protein, p50, with actin: a possible link between mRNA and microfilaments. *J. Cell Sci.*, **112**, 3487–3496.
- Bouvet, P. and Wolffe, A.P. (1994) A role for transcription and FRGY2 in masking maternal mRNA within *Xenopus* oocytes. *Cell*, **77**, 931–941.
- Matsumoto, K., Meric, F. and Wolffe, A.P. (1996) Translational repression dependent on the interaction of the *Xenopus* Y-box protein FRGY2 with mRNA. Role of the cold shock domain, tail domain, and selective RNA sequence recognition. *J. Biol. Chem.*, **271**, 22706–22712.
- Matsumoto, K., Tanaka, K.J., Aoki, K., Sameshima, M. and Tsujimoto, M. (2003) Visualization of the reconstituted FRGY2-mRNA complexes by electron microscopy. *Biochem. Biophys. Res. Commun.*, **306**, 53–58.

9. Yang, J., Medvedev, S., Yu, J., Schultz, R.M. and Hecht, N.B. (2006) Deletion of the DNA/RNA-binding protein MSY2 leads to post-meiotic arrest. *Mol. Cell Endocrinol.*, **250**, 20–24.
10. Medvedev, S., Pan, H. and Schultz, R.M. (2011) Absence of MSY2 in mouse oocytes perturbs oocyte growth and maturation, RNA stability, and the transcriptome. *Biol. Reprod.*, **85**, 575–583.
11. Mansfield, J.H., Wilhelm, J.E. and Hazelrigg, T. (2002) Ypsilon Schachtel, a Drosophila Y-box protein, acts antagonistically to Orb in the oskar mRNA localization and translation pathway. *Development*, **129**, 197–209.
12. Kumari, P., Gilligan, P.C., Lim, S., Tran, L.D., Winkler, S., Philp, R. and Sampath, K. (2013) An essential role for maternal control of Nodal signaling. *Elife*, **2**, e00683.
13. Weston, A. and Somerville, J. (2006) Xp54 and related (DDX6-like) RNA helicases: roles in messenger RNP assembly, translation regulation and RNA degradation. *Nucleic Acids Res.*, **34**, 3082–3094.
14. Boag, P.R., Nakamura, A. and Blackwell, T.K. (2005) A conserved RNA-protein complex involved in physiological germline apoptosis regulation in *C. elegans*. *Development*, **132**, 4975–4986.
15. Navarro, R.E., Shim, E.Y., Kohara, Y., Singson, A. and Blackwell, T.K. (2001) cgh-1, a conserved predicted RNA helicase required for gametogenesis and protection from physiological germline apoptosis in *C. elegans*. *Development*, **128**, 3221–3232.
16. Audhya, A., Hyndman, F., McLeod, I.X., Maddox, A.S., Yates, J.R., Desai, A. and Oegema, K. (2005) A complex containing the Sm protein CAR-1 and the RNA helicase CGH-1 is required for embryonic cytokinesis in *Caenorhabditis elegans*. *J. Cell Biol.*, **171**, 267–279.
17. Boag, P.R., Atalay, A., Robida, S., Reinke, V. and Blackwell, T.K. (2008) Protection of specific maternal messenger RNAs by the P body protein CGH-1 (Dhh1/RCK) during *Caenorhabditis elegans* oogenesis. *J. Cell Biol.*, **182**, 543–557.
18. Noble, S.L., Allen, B.L., Goh, L.K., Nordick, K. and Evans, T.C. (2008) Maternal mRNAs are regulated by diverse P body-related mRNP granules during early *Caenorhabditis elegans* development. *J. Cell Biol.*, **182**, 559–572.
19. Hubstenberger, A., Noble, S.L., Cameron, C. and Evans, T.C. (2013) Translation repressors, an RNA helicase, and developmental cues control RNP phase transitions during early development. *Dev. Cell*, **27**, 161–173.
20. de Carvalho, C.E., Zaaier, S., Smolikov, S., Gu, Y., Schumacher, J.M. and Colaiacovo, M.P. (2008) LAB-1 antagonizes the Aurora B kinase in *C. elegans*. *Genes Dev.*, **22**, 2869–2885.
21. Miller, J.C., Tan, S., Qiao, G., Barlow, K.A., Wang, J., Xia, D.F., Meng, X., Paschon, D.E., Leung, E., Hinkley, S.J. *et al.* (2011) A TALE nuclease architecture for efficient genome editing. *Nat. Biotechnol.*, **29**, 143–148.
22. Wood, A.J., Lo, T.W., Zeitler, B., Pickle, C.S., Ralston, E.J., Lee, A.H., Amora, R., Miller, J.C., Leung, E., Meng, X. *et al.* (2011) Targeted genome editing across species using ZFNs and TALENs. *Science*, **333**, 307.
23. Mihailovich, M., Militti, C., Gabaldon, T. and Gebauer, F. (2010) Eukaryotic cold shock domain proteins: highly versatile regulators of gene expression. *Bioessays*, **32**, 109–118.
24. Katic, I. and Grosshans, H. (2013) Targeted heritable mutation and gene conversion by Cas9-CRISPR in *Caenorhabditis elegans*. *Genetics*, **195**, 1173–1176.
25. Sarov, M., Murray, J.I., Schanze, K., Pozniakovski, A., Niu, W., Angermann, K., Hasse, S., Rupprecht, M., Vinis, E., Tinney, M. *et al.* (2012) A genome-scale resource for in vivo tag-based protein function exploration in *C. elegans*. *Cell*, **150**, 855–866.
26. Merritt, C., Rasoloson, D., Ko, D. and Seydoux, G. (2008) 3' UTRs are the primary regulators of gene expression in the *C. elegans* germline. *Curr. Biol.*, **18**, 1476–1482.
27. Frokjaer-Jensen, C., Davis, M.W., Hopkins, C.E., Newman, B.J., Thummel, J.M., Olesen, S.P., Grunnet, M. and Jorgensen, E.M. (2008) Single-copy insertion of transgenes in *Caenorhabditis elegans*. *Nat. Genet.*, **40**, 1375–1383.
28. Timmons, L. and Fire, A. (1998) Specific interference by ingested dsRNA. *Nature*, **395**, 854.
29. Scheckel, C., Gaidatzis, D., Wright, J.E. and Ciosk, R. (2012) Genome-wide analysis of GLD-1-mediated mRNA regulation suggests a role in mRNA storage. *PLoS Genet.*, **8**, e1002742.
30. Ding, X.C. and Grosshans, H. (2009) Repression of *C. elegans* microRNA targets at the initiation level of translation requires GW182 proteins. *EMBO J.*, **28**, 213–222.
31. Hendriks, G.J., Gaidatzis, D., Aeschmann, F. and Grosshans, H. (2014) Extensive oscillatory gene expression during *C. elegans* larval development. *Mol. Cell*, **53**, 380–392.
32. Grant, B. and Hirsh, D. (1999) Receptor-mediated endocytosis in the *Caenorhabditis elegans* oocyte. *Mol. Biol. Cell.*, **10**, 4311–4326.
33. Lewis, J.A. and Fleming, J.T. (1995) Basic culture methods. *Methods Cell Biol.*, **48**, 3–29.
34. Schmidt, E.K., Clavarino, G., Ceppi, M. and Pierre, P. (2009) SUnSET, a nonradioactive method to monitor protein synthesis. *Nat. Methods*, **6**, 275–277.
35. Hansen, M., Taubert, S., Crawford, D., Libina, N., Lee, S.J. and Kenyon, C. (2007) Lifespan extension by conditions that inhibit translation in *Caenorhabditis elegans*. *Aging Cell*, **6**, 95–110.
36. Keller, A., Nesvizhskii, A.I., Kolker, E. and Aebersold, R. (2002) Empirical statistical model to estimate the accuracy of peptide identifications made by MS/MS and database search. *Anal. Chem.*, **74**, 5383–5392.
37. Nesvizhskii, A.I., Keller, A., Kolker, E. and Aebersold, R. (2003) A statistical model for identifying proteins by tandem mass spectrometry. *Anal. Chem.*, **75**, 4646–4658.
38. Bargmann, C.I., Hartwig, E. and Horvitz, H.R. (1993) Odorant-selective genes and neurons mediate olfaction in *C. elegans*. *Cell*, **74**, 515–527.
39. Nuttley, W.M., Atkinson-Leadbetter, K.P. and Van Der Kooy, D. (2002) Serotonin mediates food-odor associative learning in the nematode *Caenorhabditis elegans*. *Proc. Natl. Acad. Sci. U.S.A.*, **99**, 12449–12454.
40. Stetak, A., Horndli, F., Maricq, A.V., van den Heuvel, S. and Hajnal, A. (2009) Neuron-specific regulation of associative learning and memory by MAGI-1 in *C. elegans*. *PLoS One*, **4**, e6019.
41. Moss, E.G., Lee, R.C. and Ambros, V. (1997) The cold shock domain protein LIN-28 controls developmental timing in *C. elegans* and is regulated by the *lin-4* RNA. *Cell*, **88**, 637–646.
42. Huang, Y. (2012) A mirror of two faces: Lin28 as a master regulator of both miRNA and mRNA. *Wiley Interdiscip. Rev. RNA*, **3**, 483–494.
43. Thieringer, H.A., Singh, K., Trivedi, H. and Inouye, M. (1997) Identification and developmental characterization of a novel Y-box protein from *Drosophila melanogaster*. *Nucleic Acids Res.*, **25**, 4764–4770.
44. Franco, G.R., Garratt, R.C., Tanaka, M., Simpson, A.J. and Pena, S.D. (1997) Characterization of a *Schistosoma mansoni* gene encoding a homologue of the Y-box binding protein. *Gene*, **198**, 5–16.
45. Salvetti, A., Batistoni, R., Deri, P., Rossi, L. and Somerville, J. (1998) Expression of DjY1, a protein containing a cold shock domain and RG repeat motifs, is targeted to sites of regeneration in planarians. *Dev. Biol.*, **201**, 217–229.
46. Hutten, S. and Kehlenbach, R.H. (2007) CRM1-mediated nuclear export: to the pore and beyond. *Trends Cell Biol.*, **17**, 193–201.
47. Thandapani, P., O'Connor, T.R., Bailey, T.L. and Richard, S. (2013) Defining the RGG/RG motif. *Mol. Cell*, **50**, 613–623.
48. Takahashi, Y., Daitoku, H., Hirota, K., Tamiya, H., Yokoyama, A., Kako, K., Nagashima, Y., Nakamura, A., Shimada, T., Watanabe, S. *et al.* (2011) Asymmetric arginine dimethylation determines life span in *C. elegans* by regulating forkhead transcription factor DAF-16. *Cell Metab.*, **13**, 505–516.
49. Andux, S. and Ellis, R.E. (2008) Apoptosis maintains oocyte quality in aging *Caenorhabditis elegans* females. *PLoS Genet.*, **4**, e1000295.
50. Skabkin, M.A., Kiselyova, O.I., Chernov, K.G., Sorokin, A.V., Dubrovin, E.V., Yaminsky, I.V., Vasiliev, V.D. and Ovchinnikov, L.P. (2004) Structural organization of mRNA complexes with major core mRNP protein YB-1. *Nucleic Acids Res.*, **32**, 5621–5635.
51. Uchiumi, T., Fotovati, A., Sasaguri, T., Shibahara, K., Shimada, T., Fukuda, T., Nakamura, T., Izumi, H., Tsuzuki, T., Kuwano, M. *et al.* (2006) YB-1 is important for an early stage embryonic development: neural tube formation and cell proliferation. *J. Biol. Chem.*, **281**, 40440–40449.
52. Liu, R., Iadevaia, V., Averous, J., Taylor, P.M., Zhang, Z. and Proud, C.G. (2014) Impairing the production of ribosomal RNA activates mammalian target of rapamycin complex 1 signalling and downstream translation factors. *Nucleic Acids Res.*, **42**, 5083–5096.

53. Ingolia, N.T., Ghaemmaghami, S., Newman, J.R. and Weissman, J.S. (2009) Genome-wide analysis in vivo of translation with nucleotide resolution using ribosome profiling. *Science*, **324**, 218–223.
54. Sherman, M.Y. and Qian, S.B. (2013) Less is more: improving proteostasis by translation slow down. *Trends Biochem. Sci.*, **38**, 585–591.
55. Wolke, U., Jezuit, E.A. and Priess, J.R. (2007) Actin-dependent cytoplasmic streaming in *C. elegans* oogenesis. *Development*, **134**, 2227–2236.
56. Baugh, L.R., Hill, A.A., Slonim, D.K., Brown, E.L. and Hunter, C.P. (2003) Composition and dynamics of the *Caenorhabditis elegans* early embryonic transcriptome. *Development*, **130**, 889–900.
57. Tadros, W. and Lipshitz, H.D. (2009) The maternal-to-zygotic transition: a play in two acts. *Development*, **136**, 3033–3042.
58. Jones, A.R., Francis, R. and Schedl, T. (1996) GLD-1, a cytoplasmic protein essential for oocyte differentiation, shows stage- and sex-specific expression during *Caenorhabditis elegans* germline development. *Dev. Biol.*, **180**, 165–183.
59. Bouvet, P., Diaz, J.J., Kindbeiter, K., Madjar, J.J. and Amalric, F. (1998) Nucleolin interacts with several ribosomal proteins through its RGG domain. *J. Biol. Chem.*, **273**, 19025–19029.
60. Lee, J.H., Pestova, T.V., Shin, B.S., Cao, C., Choi, S.K. and Dever, T.E. (2002) Initiation factor eIF5B catalyzes second GTP-dependent step in eukaryotic translation initiation. *Proc. Natl. Acad. Sci. U.S.A.*, **99**, 16689–16694.
61. Babiano, R. and de la Cruz, J. (2010) Ribosomal protein L35 is required for 27SB pre-rRNA processing in *Saccharomyces cerevisiae*. *Nucleic Acids Res.*, **38**, 5177–5192.
62. Fernandez-Pevida, A., Rodriguez-Galan, O., Diaz-Quintana, A., Kressler, D. and de la Cruz, J. (2012) Yeast ribosomal protein L40 assembles late into precursor 60 S ribosomes and is required for their cytoplasmic maturation. *J. Biol. Chem.*, **287**, 38390–38407.